Amplitude universality for driven interfaces and directed polymers in random media

Joachim Krug
IBM Research Division, Thomas J. Watson Research Center, Yorktown Heights, New York 10598

Paul Meakin
Central Research and Development, The du Pont Company, Experimental Station E356/153, Wilmington, Delaware 19880-0356

Timothy Halpin-Healy
Physics Department, Barnard College, Columbia University, New York, New York 10027-6598

(Received 5 September 1991)

We present accurate estimates for the prefactors of the second and third moments of the height and free-energy fluctuations, as well as the leading correction to the growth rate and free energy per unit length, obtained from extensive simulations of a wide range of one-dimensional models of growing interfaces and directed polymers in a random environment. When scaled by the appropriate model-dependent parameters the amplitudes reduce to universal numbers which characterize the strong-coupling fixed point of the equation of Kardar, Parisi, and Zhang [Phys. Rev. Lett. **56**, 889 (1986)]. To check the expected scaling we use models for which the model parameters can be computed analytically. For other systems, such as ballistic deposition, the restricted solid-on-solid model, and the finite-temperature directed polymer, the parameters are determined numerically from steady-state properties. Apart from the standard transient simulation which starts from a flat interface, we also report results for time-dependent correlations in the steady state, which give rise to different universal amplitudes. We compare our results with recent predictions arising from replica calculations and dynamic renormalization-group treatments, finding agreement in the latter but severe discrepancies in the former case. We speculate that the failure of replica theory may be indicative of replica symmetry breaking.

PACS number(s): 02.50.+s, 05.40.+j, 61.50.Cj, 75.60.Ch

I. INTRODUCTION

In the past five years following the seminal work of Kardar, Parisi, and Zhang (KPZ) [1] the kinetic roughening of driven interfaces has aroused a tremendous amount of interest in the statistical-physics community [2]. Indeed, the KPZ theory provides a quantitative understanding of some of the fascinating structures generated in a broad range of stochastic nonequilibrium processes [3]. Moreover, kinetic roughening is of relevance to many applied fields ranging from crystal-growth [4] and deposition [5] processes to two-phase flow in porous media [6]. Hence long-standing problems in materials science, such as the columnar growth morphology observed in thin-film deposition [7], can be expected to benefit from our improved understanding of kinetic roughening. Finally, workers with a background in the statistical mechanics of disordered systems have been attracted to the field by the close formal relation between moving interfaces and directed polymers in a random medium [8], bringing with them a wealth of powerful and inventive methods [9–12].

Here the term kinetic roughening implies the process by which the noisy local displacement dynamics of an interface translates into scale-invariant fluctuations of the interface position. In the commonly employed simulation scheme the interface is prepared in a flat state at time $t=0$ and the evolution of the fluctuations is monitored by measuring the width

$$\xi=\langle[h(\mathbf{x},t)-\langle h(\mathbf{x},t)\rangle]^2\rangle^{1/2}\ , \tag{1}$$

where $h(\mathbf{x},t)$ denotes the height of the interface above a point $\mathbf{x}$ on a d-dimensional substrate, at time t. The width grows with time as a power law up to a saturation time that scales with the substrate size L as L^z, where z is the dynamic scaling exponent. The dependence on t and L can be summarized in the scaling form [13]

$$\xi(t,L)=L^{\zeta}f(t/L^z)\ , \tag{2}$$

where the scaling function $f(x)$ saturates at large x and $f(x\to 0)\sim x^{\zeta/z}$. The width grows as $t^{\zeta/z}$ at early times and saturates at a value proportional to L^{ζ}. The exponent ζ is called the roughness or wandering [14] exponent. The two scaling exponents in (2) satisfy the relation $\zeta+z=2$ [15–17].

A specific symmetry of one-dimensional interfaces [18,19] forces the roughness exponent to take the value $\zeta=\frac{1}{2}$ familiar from thermal equilibrium, and hence $z=\frac{3}{2}$ exactly [1]. Much of the previous numerical work has focused on obtaining accurate estimates for the scaling exponents in dimensions $d=2$ and higher [20,21]. In the present paper we return to the one-dimensional case to look for universal quantities other than the scaling exponents which can be extracted from theory and simulations. Specifically, we investigate the prefactors of the asymptotic power laws governing the divergence of the interface width (1) and higher moments of the height fluctuations. Our motivation is twofold. First, in experimen-

 © 1992 The American Physical Society

tal applications [4,6] it is important to understand how these amplitudes depend on the system parameters in order to estimate the range in which to expect the asymptotic power laws. Second, since the scaling exponents in one dimension are basically determined by the symmetries of the problem, the fact that different models show the same asymptotic scaling gives only a weak indication of the presence of true universality. Technically speaking, the existence of several fixed points with identical scaling exponents is a conceivable scenario [22] in the renormalization-group context [1,11,17] which can be ruled out only by demonstration of amplitude universality.

Different sets of amplitudes are associated with the two asymptotic regimes combined in (2). Since we wish to characterize the full probability distribution of the height fluctuations, we define one set of amplitudes associated with the transient regime $t \ll L^z$,

$$a_n = \lim_{t\to\infty} \lim_{L\to\infty} t^{-n/3} \langle [h(x,t) - \langle h(x,t) \rangle]^n \rangle_c \ , \tag{3}$$

where $\langle X^n \rangle_c$ denotes the nth cumulant [23] of the random variable X, and one set associated with the stationary regime $t \gg L^z$,

$$b_n = \lim_{L\to\infty} \lim_{t\to\infty} L^{-n/2} \langle [h(x,t) - \langle h(x,t) \rangle]^n \rangle_c \ . \tag{4}$$

Comparing with (2) it is clear that $\lim_{y\to\infty} f(y) = b_2^{1/2}$ and $f(y) \approx a_2^{1/2} y^{1/3}$ for $y \to 0$. It will turn out that, due to the special structure of the one-dimensional problem, the static amplitudes b_n are trivial, while the dynamic amplitudes a_n contain nontrivial information about the KPZ fixed point.

Another quantity of interest is the leading correction to the asymptotic growth rate $v_\infty = \lim_{t,L\to\infty} \langle \partial h/\partial t \rangle$. Two of us have recently shown that [24]

$$\langle \partial h/\partial t \rangle - v_\infty = L^{-1} \tilde{f}(t/L^z) \tag{5}$$

for one-dimensional interfaces, where $\tilde{f}(y) = \text{const}$ for $y \gg 1$ and $\tilde{f}(y) \sim y^{-2/3}$ for $y \ll 1$. This leads to the amplitudes

$$a_v = \lim_{t\to\infty} \lim_{L\to\infty} t^{2/3} (\langle \partial h/\partial t \rangle - v_\infty) \tag{6}$$

and

$$b_v = \lim_{L\to\infty} \lim_{t\to\infty} L (\langle \partial h/\partial t \rangle - v_\infty) \ , \tag{7}$$

hence $b_v = \lim_{x\to\infty} \tilde{f}(y)$ and $a_v = \lim_{y\to 0} y^{2/3} \tilde{f}(y)$.

The amplitudes defined above are not universal as they stand: They contain model-dependent parameters that have to be determined in order to extract universal numbers. The relevant parameters will be identified in the next section, and it will be shown how they can be numerically measured for a given growth model. To avoid numerical uncertainties associated with the determination of these parameters, we have investigated a family of models for which they can be derived exactly. This will be described in Sec. III. Section IV summarizes our numerical estimates for the universal amplitudes. In particular, we find that all growth models belong to a single universality class. In Sec. V the connection to directed polymers in a random medium is outlined, the relevant parameters are identified, and numerical estimates of the amplitudes are presented that agree with the results obtained from the growth models. In Sec. VI we abandon the conventional setup of starting from a flat interface, and investigate instead dynamic fluctuations in the stationary regime. This leads to a different set of amplitudes. Finally in the last section we conclude by comparing our numerical results to existing theoretical predictions. Some technical details concerning the numerical measurement of the amplitude b_v defined in (7) are discussed in an appendix.

II. MODEL-DEPENDENT PARAMETERS AND UNIVERSAL AMPLITUDES

According to Kardar, Parisi, and Zhang the local position $h(\mathbf{x},t)$ of a moving interface satisfies [1]

$$\frac{\partial}{\partial t} h(\mathbf{x},t) = v_0 + \frac{\lambda}{2} (\nabla h)^2 + \nu \nabla^2 h + \eta(\mathbf{x},t) \ , \tag{8}$$

where the first two terms on the right-hand side arise from a gradient expansion of the macroscopic inclination-dependent growth rate [25] and the last two terms describe the microscopic growth-rate fluctuations. The noise η is Gaussian with zero mean and variance

$$\langle \eta(\mathbf{x},t) \eta(\mathbf{x}',t') \rangle = D \delta^d(\mathbf{x}-\mathbf{x}') \delta(t-t') \ . \tag{9}$$

The major simplifying feature in $d=1$ is that the stationary height fluctuations are *independent* of the nonlinear term in (8), and hence all static (stationary, equal time) correlation functions can be easily computed [18,19]. The stationary distribution is Gaussian, with the variance

$$\lim_{t\to\infty} \langle |\hat{h}(k,t)|^2 \rangle = \frac{D}{2\nu L k^2} \tag{10}$$

for the discrete Fourier modes $\hat{h}(k,t)$, $k = 2\pi m/L$, $m = -L/2, \ldots, -1, 1, \ldots, L/2$. Consequently, the stationary height-difference correlation function in an infinite system is

$$C_h(r) = \lim_{t\to\infty} \langle [h(x+r,t) - h(x,t)]^2 \rangle = Ar \tag{11}$$

for large r, with

$$A = \frac{D}{2\nu} \ , \tag{12}$$

and the stationary width in a finite system with periodic boundary conditions is

$$\lim_{t\to\infty} \xi(t,L) = \left[\frac{A}{12} \right]^{1/2} L^{1/2} \tag{13}$$

for large L, i.e., $b_2 = A/12$. The Gaussian character of the stationary distribution implies that all higher cumulants vanish, $b_n = 0$ for $n > 2$.

The finite-size correction (5) arises from the fluctuation contribution to the growth rate obtained by averaging the right-hand side of (8). Using (10) it follows that [24]

$$b_v = -\frac{\lambda}{2} \langle (\nabla h)^2 \rangle = -\frac{\lambda A}{2} \ . \tag{14}$$

From a practical point of view, the results (11), (13), and (14) for the static amplitudes provide us with a simple method to numerically determine the values of A and λ for any model of interest. In addition, λ can be determined directly from the inclination dependence of the growth rate. Indeed by imposing a small tilt $h(x,t)\to h(x,t)+\epsilon x$ in (8) and computing the response in the average growth rate we find [25]

$$\lambda = v''_{\infty}(0) \ . \tag{15}$$

These ideas will be put to work in Sec. IV.

In the transient regime (10) takes on the dynamic scaling form [26–28]

$$\langle |\hat{h}(k,t)|^2 \rangle = \frac{D}{2\nu L k^2} g[(\lambda^2 A)^{1/3} k t^{2/3}] \ , \tag{16}$$

where g is now a *universal* (model-independent) nontrivial scaling function. The height fluctuations in this regime are no longer expected to be Gaussian, and hence the higher moments are not related to the variance (16) in any simple way. In particular, since the nonlinear term in (8) breaks the $h \to -h$ symmetry, odd moments may become nonzero. Nevertheless the higher moments are expected to satisfy scaling relations similar to (16). Under this assumption it follows that the general form of the transient amplitudes is

$$a_n = (|\lambda| A^2)^{n/3} c_n \tag{17}$$

and

$$a_v = (|\lambda| A^2)^{1/3} c_v \ , \tag{18}$$

where the absolute values of c_n and c_v are expected to be universal numbers. The *signs* of c_n (for $n>2$) and c_v are not fixed *a priori*, but it is clear from the symmetry of (8) that they have to be determined by the (model-dependent [25]) sign of λ. It has been shown previously [24] that the sign of c_v is opposite to the sign of λ [see also (14)].

Both c_2 and c_v can be related to the scaling function g of the variance (16). Going to the continuum limit in k one obtains

$$c_2 = \frac{1}{\pi} \int_0^{\infty} dx \frac{g(x)}{x^2} \tag{19}$$

and

$$|c_v| = \frac{1}{2\pi} \int_0^{\infty} dx [1-g(x)] \tag{20}$$

[recall that $\lim_{y\to\infty} g(y)=1$ by definition]. Assuming a Gaussian shape for the scaling function, $g(x)=1-e^{-\alpha x^2}$, leads to the simple relation

$$c_2 |c_v| = \frac{1}{4\pi} \approx 0.079\,58 \tag{21}$$

independent of the width α.

The main point of these considerations is that all amplitudes can be expressed in terms of only two model parameters, the spatial correlation function amplitude A and the KPZ coefficient λ. In the context of the KPZ equation (8), this implies that the parameters ν and D appear only in the combination D/ν. The nontrivial dynamic amplitudes (17) and (18) are governed by the single scaling parameter

$$\vartheta = A^2 |\lambda| \ . \tag{22}$$

In particular, the nth cumulant diverges as $(\vartheta t)^{n/3}$ in the transient regime, with a universal prefactor c_n.

It is instructive to rederive this result from a simple argument developed previously [7,29] to demonstrate the scaling relation $\zeta+z=2$. At a given time $t \ll L^{3/2}$ the interface is rough on all scales below the dynamic correlation length $\xi_{\parallel}(t)$. At smaller scales the height fluctuations are stationary, which implies that the asymptotic form (11) of the height-difference correlation function can be used to estimate the width as $\xi^2 \approx A \xi_{\parallel}$. We consider a typical interface fluctuation, which is a hump of width $\xi_{\parallel}$ and height ξ. It is readily shown [7] that such a hump widens, under the action of the nonlinear term in the KPZ equation (8), according to

$$\dot{\xi}_{\parallel} \approx |\lambda| (\xi / \xi_{\parallel}) \tag{23}$$

which leads to $\xi_{\parallel} \approx (A^{1/2} |\lambda| t)^{2/3}$ and $\xi \approx (A^2 |\lambda| t)^{1/3}$. The same reasoning carries over to higher-dimensional interfaces, where the scaling exponents ζ and z are not known exactly. Defining the stationary amplitude A through $C_h(\mathbf{r}) = A |\mathbf{r}|^{2\zeta}$ we find $\xi_{\parallel} \approx (A^{1/2} |\lambda| t)^{1/z}$ with $z = 2-\zeta$ and, using the scaling relation, $\xi \approx (A^{1/\zeta} |\lambda| t)^{\zeta/z}$. Hence the general expression for the scaling parameter is

$$\vartheta = A^{1/\zeta} |\lambda| \ . \tag{24}$$

We note, however, that the relation between A and the parameters in the KPZ equation is not as simple as (12) in higher dimensions. In particular, A is expected to depend on λ.

III. SINGLE-STEP MODELS

It is useful for our purposes to start out with a family of models for which the parameters A and λ can be obtained analytically. The nearest-neighbor height differences (step heights) $\sigma_x = h_{x+1} - h_x$, $x = 1, \ldots, L$, in these models are restricted to the values $+1$ or -1, and hence can be conveniently thought of as "spins" [15,30]. Particles are added, $h_x \to h_x + 2$, at local minima where $(\sigma_{x-1}, \sigma_x) = (-1, 1)$, and the spins at sites $x-1$ and x are exchanged by the addition. The total magnetization is thus conserved by the dynamics. Periodic boundary conditions are used for the spins. Let $N = N_+ - N_-$ denote the excess number of $+$ spins, which is fixed by the initial configuration. The tilt of the interface is then $u = \langle \sigma_x \rangle = N/L$ and the height variables satisfy *helical* boundary conditions, $h_{L+1} = h_1 + N$. If the rate of adding particles is chosen to be equal at all eligible growth sites, it is straightforward to show [15] that all configurations with the prescribed value of N have the same weight in the steady state of the dynamics. This implies that

$$A = \langle \sigma_x^2 \rangle - \langle \sigma_x \rangle^2 = 1 - u^2 \ . \tag{25}$$

The density of growth sites is $(1-u^2)/4$ and, since the

addition of a particle increases the height by two, the inclination-dependent growth rate is given in units of the rate of particle addition by

$$v_\infty(u)=\tfrac{1}{2}(1-u^2) \tag{26}$$

so $\lambda=-1$ independent of u. Hence the simplest way to vary the scaling parameter ϑ is by tilting the surface.

Gates and Westcott [31] generalized the single-step model by allowing the growth rate at a given local minimum $(\sigma_{x-1},\sigma_x)=(-1,1)$ to depend on the neighboring spins σ_{x-2} and σ_{x+1}. Specifically, the rates corresponding to the various local spin configurations are given by

$$\begin{aligned} R(1,-1,1,-1)&=\min(1,e^{\beta}) \\ R(-1,-1,1,1)&=\min(1,e^{-\beta}) \\ R(-1,-1,1,-1)&=R(1,-1,1,1) \\ &=\tfrac{1}{2}[R(1,-1,1,-1) \\ &\quad +R(-1,-1,1,1)] . \end{aligned} \tag{27}$$

This choice of rates guarantees that the steady state of the spin system is the Gibbs state of the one-dimensional Ising model at reduced inverse temperature $|\beta|$ [31,32]. The Ising model is ferromagnetic for $\beta>0$ and antiferromagnetic for $\beta<0$. For large positive β the spins are strongly correlated and the interface consists of large stretches of constant slope, i.e., extended hills and valleys [Fig. 1(a)]. Similarly for large negative β the interaction makes the interface rather flat [Fig. 1(b)]. This is reflected in the simple result for the stationary correlation function amplitude at zero tilt [31]

$$A=e^{\beta/2} . \tag{28}$$

The growth rate at zero tilt is given by [31]

$$v_\infty=\frac{e^{-|\beta|/2}}{1+e^{\beta/2}} . \tag{29}$$

Using the Ising steady state the inclination dependence of both A and v_∞ can be worked out [33]. The resulting variation of λ with β is shown in Fig. 2. It should be noted that λ changes sign at $\beta=\beta_c=-2\ln(3)$. Similar behavior has been found in other growth models [34].

It is evident from Fig. 2 that the regimes of large positive and negative β are qualitatively different in the sense that $A\gg1\gg\lambda$ for $\beta\gg1$ while $A\ll1\ll\lambda$ for $\beta\ll-1$. On the other hand, the variation in the scaling parameter ϑ is rather modest for reasonable values of β. In the limit $\beta\to-\infty$ the dynamics reduces [31] to the polynuclear

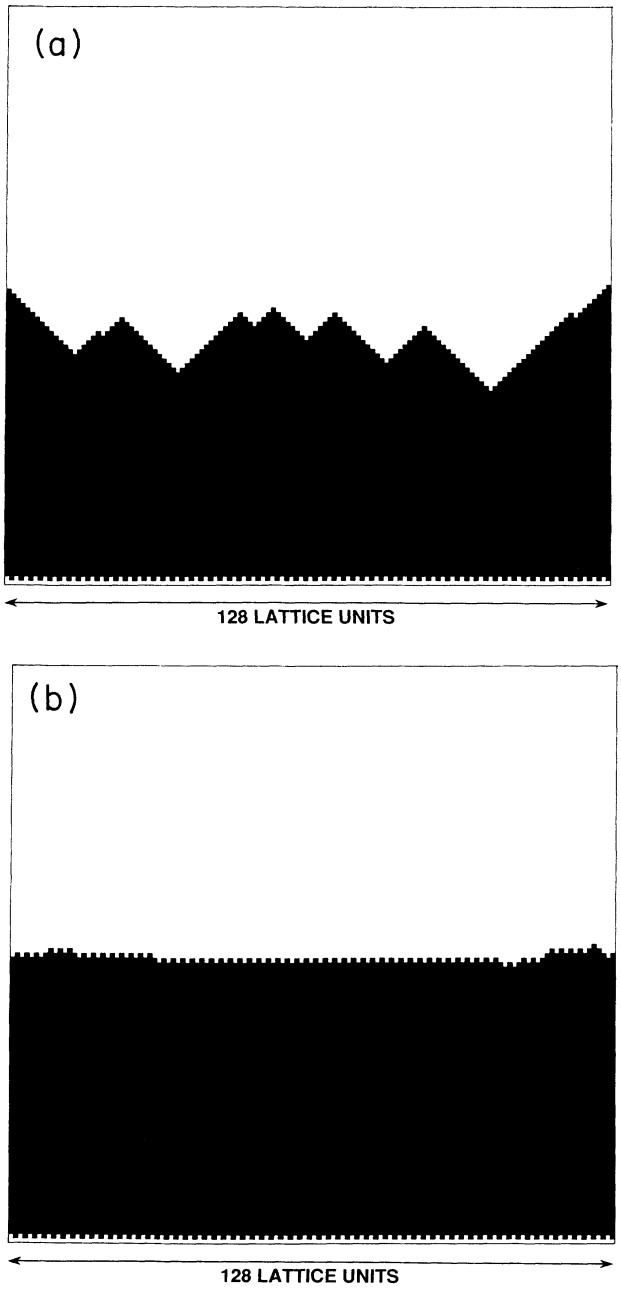

FIG. 1. Interface structures obtained from small-scale simulations carried out to illustrate the model of Gates and Westcott [31]. (a) The strongly ferromagnetic case ($\beta=4$) and (b) the strongly antiferromagnetic case ($\beta=-4$).

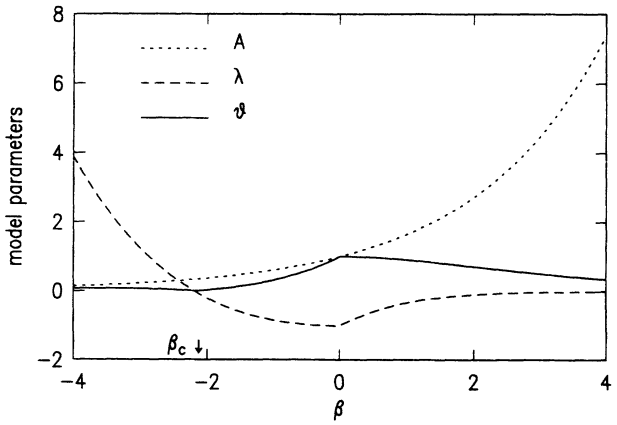

FIG. 2. Analytical results for the static correlation-function amplitude A, the KPZ coefficient λ and the scaling parameter $\vartheta=A^2|\lambda|$ of the Gates-Westcott model. The transition point β_c where λ goes through zero is indicated by an arrow.

growth (PNG) model [35], in which islands nucleate at a rate $p \approx e^{\beta} \ll 1$ and then grow sideways at unit speed. The regime of large negative β is therefore more efficiently accessed by directly simulating a discretized [36] PNG model. In the limit of small nucleation rate it can be shown [36] that $A = \sqrt{2p}$ and $\lambda = 1/\sqrt{2p}$, hence

$$\vartheta = \sqrt{2p} \ , \tag{30}$$

which can be made arbitrarily small. In practice, p is limited by the requirement that the average step spacing $l \approx 1/A$ remain small compared to the substrate size.

IV. NUMERICAL RESULTS FOR GROWTH MODELS

In addition to the models discussed in the preceding section, we have investigated the restricted solid-on-solid (RSOS) model of Kim and Kosterlitz [20], and square-lattice ballistic deposition with sticking at nearest-neighbor (NN), and nearest as well as next-nearest-neighbor (NNN) columns [15]. For these models A was determined numerically from the stationary height-difference correlation function (11), and λ was extracted from the stationary velocity-correction amplitude (14) using the numerically determined value of A, i.e., the scaling parameter (22) was defined through $\vartheta = 2A|b_v|$. Examples of the kind of data we have used are shown in Fig. 3. The results are summarized for future reference in Table I. We also include estimates of λ obtained by directly measuring the inclination dependence of the growth rate [25]. The value of A can alternatively be determined from the stationary width amplitude (13), which gives identical results within the statistical uncertainties.

These uncertainties vary substantially from model to model. Quite accurate values for A and λ, which are in excellent agreement with the analytical results presented in Sec. 3, can be obtained from the Gates-Westcott model for small values of β. For the RSOS model we estimate that the uncertainties in A and λ are less than $\pm 10\%$. For the NN and NNN ballistic deposition models it is much more difficult to approach the asymptotic ($t \to \infty, L \to \infty$) limit and the uncertainties are larger than $\pm 10\%$, even for simulations in which as many as 5×10^{10} particles are deposited.

There is a subtle time-scale effect involved in measuring the stationary velocity-correction amplitude for reaction limited models [25] (such as the single-step models and the RSOS model), which is discussed in the Appendix. In general, however, the choice of time scale (which is largely arbitrary for the models of interest here) does not affect the estimation of the amplitudes (3) and (6), as long as the choice is made consistently for *all* measurements on a given model. The reason is that time t appears in the combination λt in all observable quantities [cf. (17) and (18)]. Since λ is the second derivative of the growth rate with respect to inclination, cf. (15), any rescaling of time rescales the growth rate and hence λ as well, leaving λt invariant.

The cumulant amplitudes (3) were measured in simulations on very wide substrates (up to $L = 2^{21} = 2\,097\,152$) in order to avoid saturation effects. In some cases better scaling was achieved by using many (typically 200) independent runs on smaller substrates ($L = 10\,000$). The number of particles added during a simulation ranged from 2×10^9 for the PNG model up to 5×10^{10} for NNN ballistic deposition. We have taken care to only use data that were as far as possible within the asymptotic scaling region, since otherwise large uncertainties in the amplitudes result. In particular, this has prevented us from exploring the region close to the critical point $\beta = \beta_c$ of the Gates-Westcott model (cf. Sec. III), where λ vanishes and therefore the time required to reach the asymptotic regime diverges. An example of the data used to determine a_2 and a_3 is shown in Fig. 4(a). In determining the finite-size correction amplitude (6) we have used the fact that the asymptotic growth rate v_∞ is known exactly for the single-step models (cf. Sec. III). For the other models a_v is determined by adjusting the asymptotic growth rate v_∞ to optimize the expected scaling (5) of the correction [Fig. 4(c)]. Alternatively a linear fit of the time-averaged growth rate $\langle h \rangle / t$ versus $t^{-2/3}$ can be used [Fig. 4(b)].

Our results for the Gates-Westcott model are shown in Fig. 5. The second-cumulant amplitude was measured in

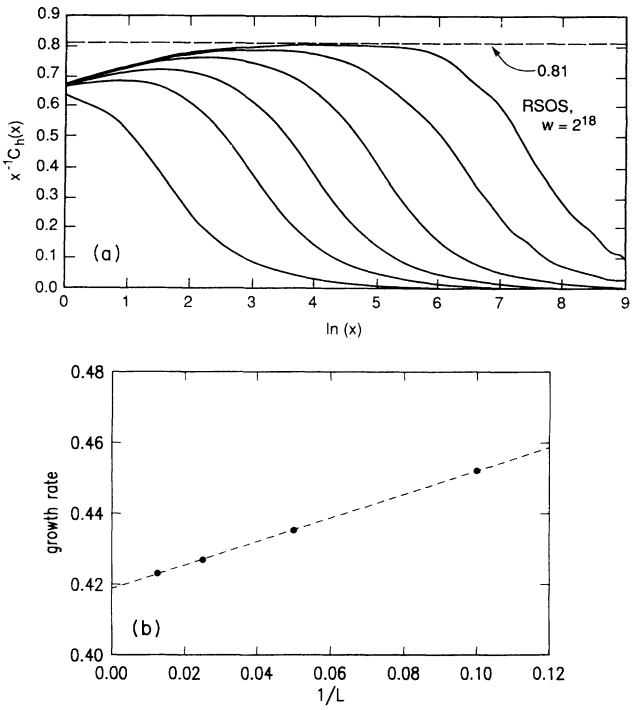

FIG. 3. Measurement of the static amplitude A and the coefficient λ for the restricted solid-on-solid model [20] with a maximal nearest-neighbor height difference of unity. (a) The determination of A from the height-difference correlation function $C_h(x)$ defined in Eq. (11), on a substrate of size $2^{18} = 262\,144$. The asymptotic behavior $C_h \sim x$ has been divided out. The correlation function is shown at six stages during the deposition process. The dashed horizontal line indicates the value estimated for A. (b) The stationary growth rate as a function of the inverse system size. The dashed line indicates a linear least-squares fit to the data, the slope of which yields our estimate for $b_v = -A\lambda/2$. Each data point corresponds to between 2×10^7 and 2×10^8 attempted depositions.

TABLE I. Numerical estimates of model parameters. A was determined from the stationary height-difference correlation function, $\lambda^{(1)}$ is an estimate using the stationary growth-rate correction amplitude, and $\lambda^{(2)}$ was obtained from the inclination dependence of the growth rate. v_∞ is the asymptotic growth rate at zero tilt, in units of one (attempted) deposition per substrate site.

Model	v_∞	A	$\lambda^{(1)}$	$\lambda^{(2)}$	ϑ
Restricted SOS	0.419	0.81	−0.81	−0.75	0.53
NN ballistic deposition	2.14	2.46	1.54	1.30	9.37
NNN ballistic deposition	4.06	6.76	1.21	1.36	55.4

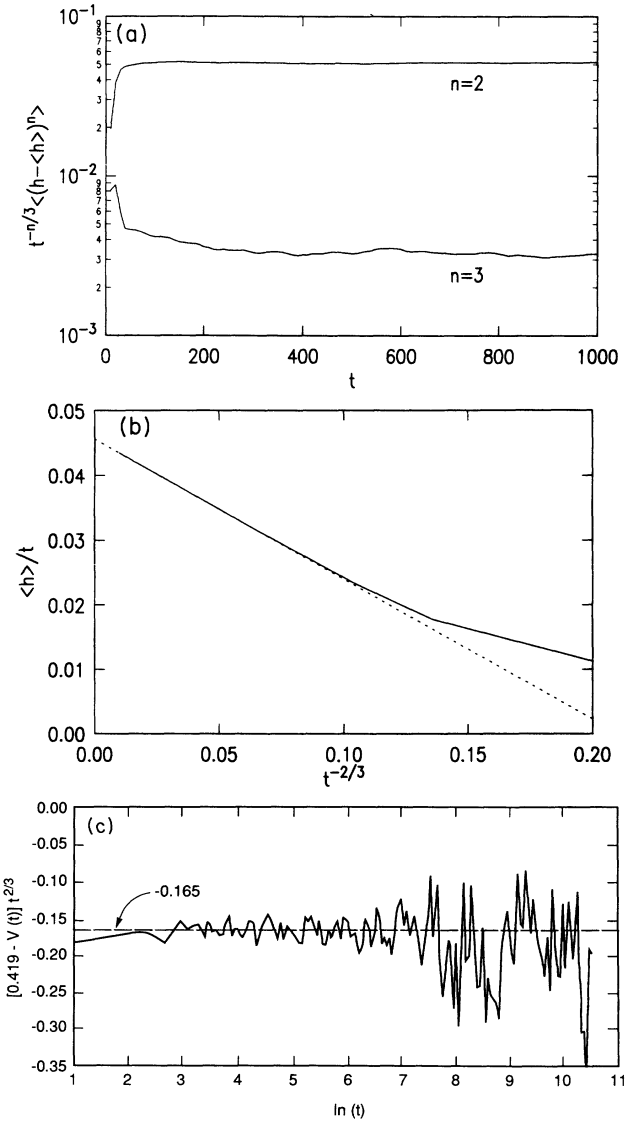

FIG. 4. Examples of simulation data used to estimate transient amplitudes. (a) Results for the second and third height fluctuation cumulant of the discrete time PNG model [36] with a nucleation probability of $p=0.001$. The predicted time dependence has been divided out. The data were obtained by averaging over 250 independent runs on a lattice of size 10 000. (b) The integrated growth rate $\langle h \rangle / t$ vs $1/t^{2/3}$, obtained from the same set of simulations. The dotted line indicates a linear least-squares fit used to estimate the amplitude a_v. (c) The momentary growth rate for the restricted solid-on-solid model on a lattice of size 2^{18}. The asymptotic growth rate v_∞ is adjusted to optimize the $t^{-2/3}$ scaling of the correction, and the estimate $a_v \approx 0.165$ is indicated by the dashed line.

the range $-4 \le \beta \le 4$, while reliable estimates for the correction amplitude a_v could be obtained only for $-1 \le \beta \le 1.5$. Figure 6 summarizes all our simulation results for c_2. We find strong evidence for universality over almost four decades in the scaling parameter $\vartheta = A^2|\lambda|$, and we estimate

$$c_2 = 0.404 \pm 0.013 \ . \tag{31}$$

Figure 7 shows the actually measured values of a_2, $|a_3|$, and $|a_v|$ in a log-log plot to demonstrate the scaling with θ predicted by (17) and (18). From the data shown we estimate

$$|c_v| = 0.193 \pm 0.013 \tag{32}$$

yielding $c_2|c_v| \approx 0.077$ in close, but possibly fortuitous, agreement with the approximate relation (21). The sign of c_3 is observed to be *equal* to the sign of λ in all cases, and the magnitude is

$$|c_3| = 0.071 \pm 0.005 \ . \tag{33}$$

Finally we quote an estimate of the fourth-cumulant amplitude obtained from a simulation of the single-step model at zero tilt,

$$c_4 = 0.02 \pm 0.002 \ . \tag{34}$$

Since $\lambda < 0$ for the single-step model, this implies that the sign of c_4 is the *opposite* of the sign of λ in general.

A useful measure of the asymmetry of the height fluctuation distribution is the *skewness* [37,38]

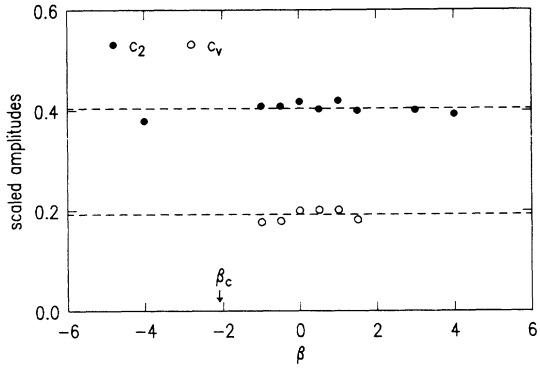

FIG. 5. Numerical results for the reduced amplitudes c_2 and c_v obtained from simulations of the Gates-Westcott model at various values of β. The dashed lines indicate our best estimates for the amplitudes, obtained by averaging the results from all models. We have not included data from the neighborhood of the transition point β_c due to the strong crossover effects observed there.

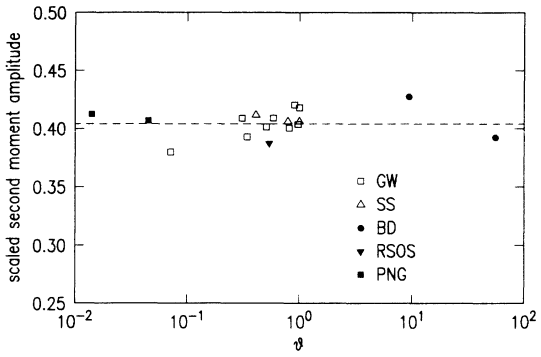

FIG. 6. Numerical results for the reduced amplitude of the second cumulant, obtained from simulations of the Gates-Westcott (GW) model, the single-step model at various values of the tilt u (SS), two versions [15] of ballistic deposition (BD), the restricted solid-on-solid model with unit maximal height difference (RSOS), and the discrete time PNG model with nucleation probability $p=0.001$ and 0.0001 (PNG). The dashed line is our best estimate for c_2.

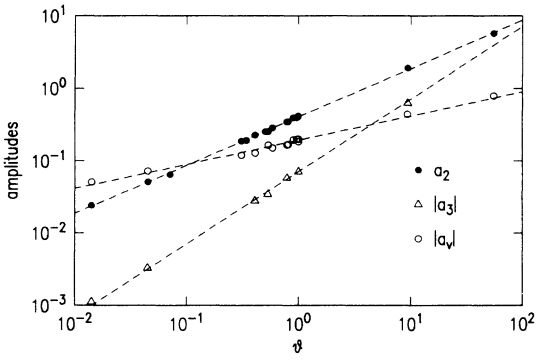

FIG. 7. Summary of numerical estimates for the cumulant amplitudes a_2 and $|a_3|$, and the finite-size correction amplitude $|a_v|$, plotted as a function of $\vartheta=A^2|\lambda|$. The dashed lines indicate the predicted power laws $a_n=c_n\vartheta^{n/3}$, $a_v=c_v\vartheta^{1/3}$ with our best values for c_n and c_v.

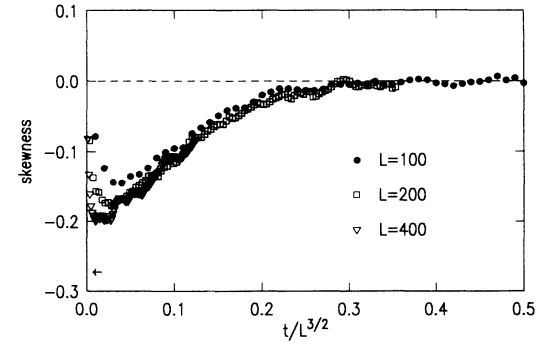

FIG. 8. Skewness of the height fluctuation distribution in the single-step model for small system sizes. The data constitute an average over 10 000 independent runs. The arrow indicates the value of the skewness in the limit $L\to\infty$.

$$s=\frac{\langle (h-\langle h\rangle)^3\rangle}{\langle (h-\langle h\rangle)^2\rangle^{3/2}} \tag{35}$$

which we estimate from (31) and (33) to take the value

$$|s|=0.28\pm0.04 \tag{36}$$

in the transient regime. We noted in Sec. II that the height fluctuations are Gaussian in the stationary regime, and hence the skewness (as well as all higher cumulants) is expected to vanish for $t\gg L^{3/2}$. It is then natural to conjecture a scaling form

$$s(t,L)=f_s(t/L^{3/2}) , \tag{37}$$

where $|f_s(0)|$ is given by (36) and $\lim_{y\to\infty}f_s(y)=0$. Similar behavior was found previously in a deterministic growth model [38]. In Fig. 8 we show numerical data for the skewness in small systems. In spite of severe finite-size effects which prevent the skewness from reaching the predicted short-time maximum value (36), there is clear indication of the dynamic-scaling form (37).

V. DIRECTED POLYMER AMPLITUDES

Closely related to the dynamic scaling properties of the stochastic-growth models discussed above are the equilibrium statistical mechanics features of finite-temperature directed polymers in random media (DPRM) [1,8]. In its discrete realization [39] for one transverse dimension ($d=1$), which we have used in the numerical simulations discussed below, the finite temperature DPRM involves a directed walk that commences at the origin of a square lattice and proceeds upwards into the half plane $t>0$, one step at a time. The vertical bonds have uncorrelated random energies $\mu(x,t)$ drawn from a uniform distribution of width Δ and variance $\sigma^2=\Delta^2/12$, while the horizontal bonds have a fixed energy cost E_0, with associated Boltzmann weight $\gamma=e^{-E_0}$ (both E_0 and μ are measured in units of kT). Consequently, a transverse step to the left or right to take advantage of a particularly favorable vertical random bond incurs a penalty $\gamma<1$. For reasons of numerical convenience, we operate under the assumption that the temperature, though finite, is relatively low so that only single steps are allowed. The transfer-matrix method permits us to investigate numerically the full partition function of the DPRM by calculating recursively the Boltzmann weight $Z(x,t)$ of paths running from the origin to the point (x,t) in the time slice t,

$$Z(x,t+1)=e^{-\mu(x,t)}[Z(x,t)+\gamma Z(x-1,t)+\gamma Z(x+1,t)] \tag{38}$$

assuming the initial condition $Z(x,0)=\delta_{x,0}$. The full partition function $\mathcal{Z}(t)$ is then obtained by summing over x,

$$\mathcal{Z}(t)=\sum_x Z(x,t) . \tag{39}$$

The quantities of immediate physical interest are the geometric and free-energy fluctuations. The former concern the disorder-induced transverse fluctuations exhibited by the directed paths as they meander through the

random energy landscape. These fluctuations are characterized by the wandering exponent [14] $\zeta_{\rm DP}$, through the relation

$$\langle x^2(t)\rangle^{1/2}\sim t^{\zeta_{\rm DP}} . \tag{40}$$

Our convention here is that thermal averages with respect to the Boltzmann weights are implicit and done first, while angular brackets denote disorder averages taken over many realizations of randomness. It is well established [9,19] that $\zeta_{\rm DP}=\frac{2}{3}$ for the case of one transverse dimension. The free-energy fluctuations, given by the disorder average of $\mathcal{F}=-\ln Z$, scale with a different exponent,

$$\langle[\mathcal{F}(t)-\langle\mathcal{F}(t)\rangle]^2\rangle^{1/2}\sim t^{\omega} , \tag{41}$$

where it is known [8,16,40] that $\omega=2\zeta_{\rm DP}-1$. The rms fluctuations (40) and (41) were first studied numerically by Huse and Henley [40], as well as Kardar [39]. Recent work by Halpin-Healy [42] has addressed the much broader question of the full geometric and free-energy probability distributions responsible for these and higher moments. A surprising feature of this recent work was the uncovering of an asymmetric free-energy distribution [43] that underlies the unique third-cumulant scaling associated with the $d=1$ DPRM. Predicted by Kardar [9] and observed by Halpin-Healy [42], this third-cumulant scaling lies at the heart of the matter, fixing the free-energy fluctuation exponent at $\omega=\frac{1}{3}$. In an effort to test the predictions made by Kardar [9] and more recently by Bouchaud and Orland [41] (BO), to be discussed in detail in Sec. VII, and to explore issues of amplitude universality, we have performed a series of finite-temperature simulations for various values of γ and Δ, studying paths of length 500 steps and typically averaging over 10^4 realizations of the random-energy landscape.

In contrast to the discrete microscopic model just delineated, the continuum formulation of the DPRM centers on the path-integral statement of the partition function,

$$Z(x,t)=\int_{y(0)=0}^{y(t)=x}\mathcal{D}y(s)\exp\left[-\int_0^t ds\left[\frac{1}{4\Gamma}\dot{y}^2-\mathcal{V}(y(s),s)\right]\right] , \tag{42}$$

where one sums explicitly over all directed paths emanating from the origin and ending at the point (x,t). The pinning potential $\mathcal{V}$ has zero mean and variance

$$\langle\mathcal{V}(x,t)\mathcal{V}(x',t')\rangle=V^2\delta(x-x')\delta(t-t') . \tag{43}$$

Here Γ is a macroscopic diffusion constant and V^2 measures the strength of the quenched randomness. In a sense to be made clear below, these parameters are renormalized versions of γ and σ^2, respectively. The partial unraveling of the precise relationship between these renormalized and microscopic parameters was a secondary interest of the present work. To establish the connection to the KPZ equation, recall that the restricted partition function $Z(x,t)$ obeys a Euclidean-time Schrödinger equation with a time-dependent random potential $\mathcal{V}$. A simple substitution [1,19] then reveals that it is the restricted free energy $F(x,t)=-\ln Z(x,t)$ that satisfies the KPZ equation (8), with the parameters

$$\nu=\Gamma , \quad \lambda=-2\Gamma , \quad D=V^2 , \tag{44}$$

and the exponents defined in (40) and (41) are related to those of the interface (cf. Sec. I) by $\zeta_{\rm DP}=1/z$, $\omega=\zeta/z$. Note that the sign of λ is fixed to be *negative* for the DPRM. The central scaling parameter (22) is given by

$$\vartheta=\frac{V^4}{2\Gamma} , \tag{45}$$

a result derived by BO directly from the partition function (42).

The major difference between the height $h(x,t)$ of the growing interfaces discussed in the preceding sections and the restricted free energy $F(x,t)$ lies in the initial condition $Z(x,0)=\delta(x)$ for the DPRM, which corresponds to a deep narrow groove in the interface [44]. Conversely, the substrate initial condition $h(x,0)=0$ corresponds, in the context of the DPRM, to an ensemble of paths emanating from *all* points x rather than just from the origin [45]. Let $\tilde{Z}(x,t)=\exp[-h(x,t)]$ denote the restricted partition function for the DPRM with substrate initial condition. $\tilde{Z}(x,t)$ gives the total weight of all paths with end point (x,t) and *arbitrary* starting point. Clearly this quantity is identical, in a statistical sense, to the weight of all paths with arbitrary end points and fixed origin, i.e., the full partition function $\bar{Z}(t)$ [Eq. (39)]. Hence we conclude that the height fluctuations studied earlier in this paper should correspond *quantitatively* to the fluctuations of the full free energy $\mathcal{F}$ of the DPRM [46]. In particular, we expect a finite-size correction to the average free energy per unit length (cf. Sec. II)

$$\langle\mathcal{F}(t)\rangle/t=f_0+\frac{3c_v\vartheta^{1/3}}{t^{2/3}} \tag{46}$$

with $c_v>0$. A similar correction, however with the opposite sign, was derived by BO [41,47].

The difficulty that forces itself upon the simulator desiring to test the concept of amplitude universality in the DPRM concerns the "correct" values of V^2 and Γ to substitute into (45). BO were, of course, aware of this subtlety, but they assumed a very simple relationship between these renormalized quantities and the microscopic input parameters of the numerical simulation, viz., $\Gamma=\gamma/3$ and $V^2=\sigma^2$, which gave, rather fortuitously in retrospect, very heartening results for some early simulations. Nevertheless, it is clear that such an assumption, though perhaps natural, is unlikely to be correct—a fact that is made apparent in the more extensive simulations that we have done.

The *proper* extrication of the renormalized diffusion constant Γ and disorder strength V^2 necessitates numeri-

cal scrutiny of the logarithm of the positional probability distribution

$$P(x,t)=\frac{Z(x,t)}{Z(t)} \ . \tag{47}$$

As pointed out by Parisi [48], and then by BO, this distribution has the properties that

$$\langle \ln[P(x,t)/P(0,t)] \rangle = -\frac{x^2}{4\Gamma t} \tag{48}$$

and

$$\langle \{\ln[P(x,t)/P(0,t)]\}^2 \rangle - \langle \ln[P(x,t)/P(0,t)] \rangle^2 = \frac{V^2}{2\Gamma}|x| \ . \tag{49}$$

In fact, these relations follow rather naturally from the mapping to the KPZ equation. Recall that $\ln[P(x,t)/P(0,t)]=-[F(x,t)-F(0,t)]$, where the restricted free energy F can be viewed as an interface evolving according to (8). The "groove" initial condition $P(x,t)=\delta(x)$ evolves, under the action of (8) with a *negative* value of λ, into a parabola given precisely by (48) [50]. Moreover, since $F(x,t)-F(0,t)$ is constrained to vanish at $x=0$, its fluctuations increase linearly with x, as predicted by the KPZ height-difference correlation function (11) [note that $V^2/2\Gamma=D/2\nu=A$ according to (44)]. It is also clear from the scaling properties of the interface [2] that the linear increase of (49) only persists on length scales less than the dynamic correlation length, $x \ll t^{2/3}$, a fact that was noticed numerically by Mézard [49], who has already provided qualitative confirmation of relations (48) and (49). Here we will rely upon them in a *quantitative* sense to determine the macroscopic parameters of the continuum model.

Consider, for example, the finite-temperature DPRM numerical experiment that we performed with input microscopic parameters $\gamma=0.1, \sigma^2=0.833$. In Fig. 9, we collect the plots which allow us to ascertain the renormalized quantities Γ and V^2, the latter being the more stubborn of the two to pin down precisely. Figure 9(a) shows data collapse to a parabola for the time slices $t=100$, 200, and 500, as expected, where we have used the scaled variable $x/2t^{1/2}$ as the abscissa. With this choice, it is a simple matter to bracket the collapsed data by appropriately scaled curves. The inner parabola corresponds to a value of $\Gamma=0.09$, while the outer has 0.10. Thus, we estimate $\Gamma(\gamma=0.1,\sigma^2=0.833)=0.095\pm0.005$, in rather strong disagreement with the BO assumption that $\Gamma=\gamma/3$. In fact, our simulations show a distinct dependence of Γ on σ^2 at fixed γ (cf. Table II), indicating that no such simple proportionality holds. Figure 9(b) examines the second moment for the same three time slices. From Eq. (49) we see that the anticipated behavior is that of the absolute-value function. For values of x that are not too large, the data conform to this notion, and the tangent line yields the slope $A=3.0$, so that $V^2=2\Gamma A \approx 0.57$. With the renormalized parameters thus determined for our particular simulation, we find that the scaling parameter has the value $\vartheta=V^4/2\Gamma \approx 1.71$. This number in hand, we can now discuss properly the issue of free-energy amplitude universality in the one-dimensional DPRM.

In Fig. 10, we plot $\langle \mathcal{F} \rangle / t$ versus $t^{-2/3}$, which shows the effects of finite size upon the free energy per unit length, cf. Eq. (46). In the thermodynamic limit we observe $f_0=-0.49$ for $\gamma=0.1$ and $\sigma^2=0.833$. Kardar [9] has invoked the replica trick to compute the quenched averaged free energy from the continuum partition function (42). He finds

$$f_0=\langle \mu \rangle - 2\Gamma - \frac{V^2}{2}+\frac{V^4}{48\Gamma} \ , \tag{50}$$

leading to $f_0 \approx -0.40$ for the case of Fig. 10. A look at the results for other parameter values collected in Table II reveals no correlation between the numerical estimates for f_0 and the formula (50). This is not entirely surprising, as the replica calculation involves [41,48,49] renormalizing the free energy by a cutoff-dependent, additive constant which arises from the self-interaction of replicas. While f_0, therefore, does not carry any universal information, the data shown in Table II do provide some insight into its general parameter dependence.

Returning to Fig. 10, we note that the free energy approaches its thermodynamic limit from *above*, consistent with the fact that $\lambda<0$ in the equivalent KPZ equation but in disagreement with the prediction of BO. The drawn tangent has slope 0.60 ± 0.01, providing us with an estimate of the amplitude of the finite-size correction. Similar data collected in Table II reveal that this amplitude is universal for a broad range of microscopic input parameters (ϑ varies from 0.17 to 179), with a value which we estimate to be

$$c_v^{\mathrm{DP}}=0.180\pm0.014 \tag{51}$$

in rather nice agreement with the numerical value (32) obtained from the growth-model simulations.

Figure 11 monitors the behavior of the amplitudes of the second and third cumulants of the free energy as a function of path length for the numerical simulation discussed above, with $\gamma=0.1$ and $\sigma^2=0.833$. As is evident from the figure, the quality of the data is such that it is possible to estimate these coefficients with rather high precision. For example, we find that asymptotically $\langle (\mathcal{F}-\langle \mathcal{F} \rangle)^2 \rangle / t^{2/3}=0.581\pm0.002$. Since this amplitude is to be identified with $a_2=\vartheta^{2/3}c_2$, while $\vartheta \approx 1.71$, we have $c_2 \approx 0.406$ for this particular set of microscopic input parameters. A glance at Table II shows that runs made for other values of γ and σ^2 yield values consistent with these, leading us to estimate

$$c_2^{\mathrm{DP}}=0.400\pm0.057 \tag{52}$$

for the universal amplitude of the second cumulant, in

TABLE II. Numerical results from finite-temperature DPRM simulations. See text for explanations.

γ	σ^2	Γ	V^2	ϑ	f_0	c_v	c_2	s
0.0125	0.833	0.026	0.395	3.00	−0.27	0.20	0.50	−0.32
	3.33	0.046	1.84	36.8	−0.94	0.17	0.35	−0.29
	8.93	0.053	2.86	77.2	−1.60	0.18	0.37	−0.32
	13.33	0.056	4.48	179	−2.68	0.19	0.35	−0.28
0.1	0.208	0.086	0.17	0.168	−0.28	0.16	0.45	−0.27
	0.833	0.095	0.57	1.71	−0.49	0.17	0.41	−0.33
	3.33	0.105	1.68	13.44	−1.16	0.19	0.37	−0.26

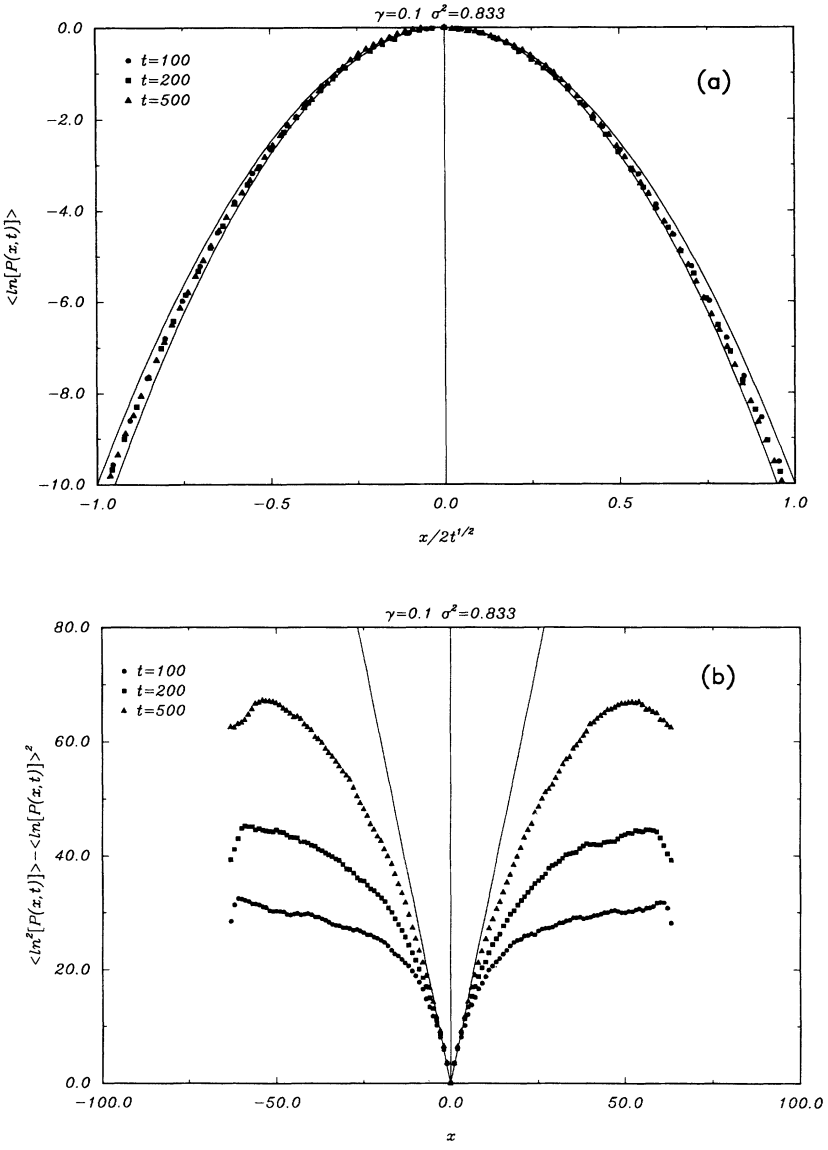

FIG. 9. (a) Disorder average of the logarithm of the spatial probability distribution $P(x,t)$ for the DPRM in $d=1$ (500 steps, 10^4 realizations of the random-energy landscape) with microscopic parameters $\gamma=0.1$ and $\sigma^2=0.833$; data collapse for the three time slices $t=100$, 200, and 500. The inner parabola corresponds to $\Gamma=0.090$, while the outer has $\Gamma=0.10$. We estimate $\Gamma(\gamma=0.1,\sigma^2=0.833)=0.095\pm0.005$. (b) Second cumulant of $\ln P(x,t)$ for the same time slices. The solid line corresponds to the function $3|x|$, which implies $A=3.0$, so that $V^2=0.57$. Together, the figures permit us to estimate $\vartheta=(V^4/2\Gamma)\approx 1.71$ for the given microscopic input parameters.

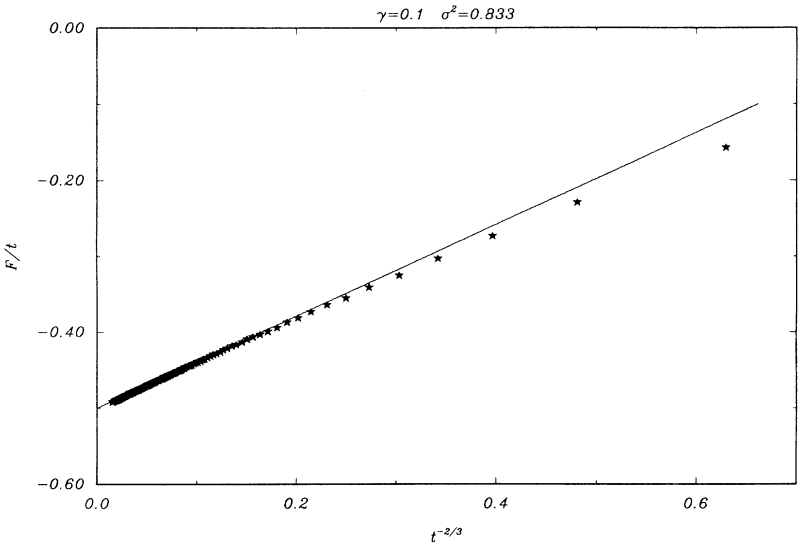

FIG. 10. Finite-size correction to the free energy per unit length of the one-dimensional DPRM vanishes as $t^{-2/3}$. The slope of the asymptotic tangent line is our estimate of the *finite-size effect* amplitude a_v for the particular simulation done here, with $\gamma=0.1$ and $\sigma^2=0.833$.

good agreement with the growth-model result (31).

Returning to Fig. 11, we note that the third cumulant is negative, in accord with the general relation between the sign of c_3 and the sign of the KPZ coefficient λ found for the growth models. The data for the third cumulant are a bit noisier than for the second. Nevertheless, we find that for large t, $\langle(\mathcal{F}-\langle\mathcal{F}\rangle)^3\rangle/t\approx-0.145\pm0.005$, which yields the estimates $c_3\approx-0.085$ and $s\approx-0.33$ for the skewness (35) of the free-energy probability distribution. In the final column of Table II, we collect our results for this skewness parameter. Figure 12 actually illustrates the behavior of this quantity as a function of path length for these runs as well as some additional ones that we made for the express purpose of pinning down s. Overall, our estimate for the skewness is

$$s^{\mathrm{DP}}=-0.296\pm0.028\ . \tag{53}$$

We have also included in Fig. 12 data for a typical zero-temperature simulation of the DPRM, which exhibits a skewness of similar magnitude in the distribution of the ground-state energy.

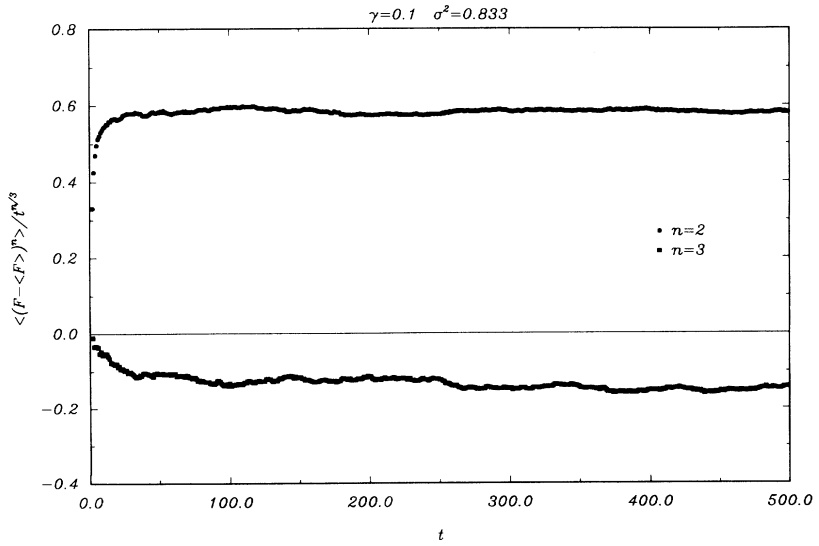

FIG. 11. Amplitudes of the second- and third-order cumulants of the free energy as a function of path length for the DPRM. Same microscopic input parameters as in previous figures. Asymptotically, $\langle(\mathcal{F}-\langle\mathcal{F}\rangle)^2\rangle/t^{2/3}$ goes to 0.581 ± 0.002, which is our estimate for a_2. Dividing by $\vartheta^{2/3}$ gives ≈0.406, which is our estimate for the *second-cumulant* universal amplitude c_2. Note that the third-order cumulant has a smaller amplitude, with $\langle(\mathcal{F}-\langle\mathcal{F}\rangle)^3\rangle/t$ approaching -0.145 ± 0.005 for large times. The relative sizes of the cumulants provide a measure for the skewness of the free-energy probability distribution.

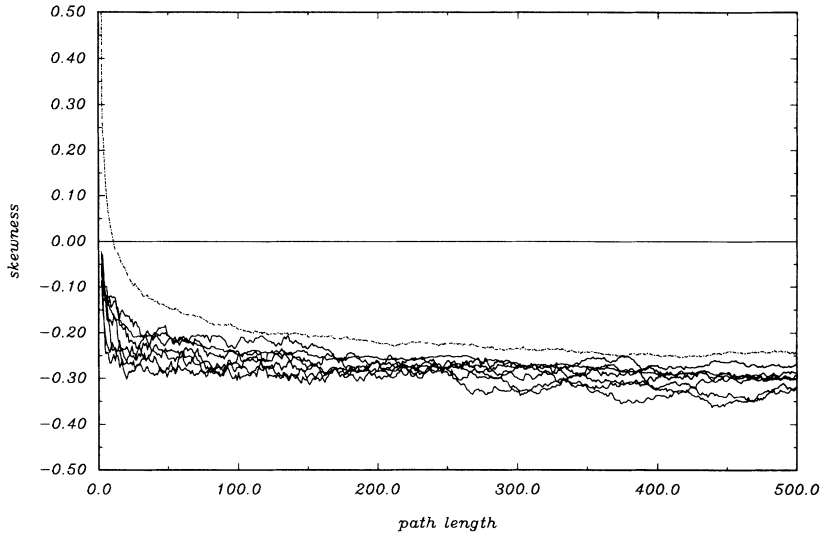

FIG. 12. *Skewness* of the free-energy probability distribution for the finite-temperature DPRM as measured by the parameter $s=\langle(\mathcal{F}-\langle\mathcal{F}\rangle)^3\rangle/\langle(\mathcal{F}-\langle\mathcal{F}\rangle)^2\rangle^{3/2}$, for simulations done with various values of γ and σ^2. We estimate $s=-0.296\pm0.028$. The uppermost curve, which is dot-dashed, shows data for the zero-temperature version of the model [8].

VI. DYNAMIC CORRELATIONS IN THE STEADY STATE

The nontrivial scaling properties of the KPZ equation (8) manifest themselves both in the roughening of an initially flat interface and in the dynamic correlations of an interface with fully developed roughness which has been growing for a time $t \gg L^z$. This latter case has received much less attention, mainly due to the numerical difficulties associated with reaching the stationary regime for large systems; it may also be of somewhat questionable physical relevance. However, the dynamic correlations in the stationary state are more easily accessible to analytic approaches starting from (8) than transient correlations involving the flat initial state, and some nontrivial amplitudes can be predicted by mode-coupling and renormalization-group calculations [27,28,51]. We have therefore performed simulations of stationary interfaces using the single-step model [15,30], where the generation of stationary configurations is trivial: Indeed, since the height differences are independent in the stationary state it is sufficient to randomly distribute spins $\sigma_i=\pm1$ on the lattice such that the total magnetization takes on a prescribed value (cf. Sec. III). There is no need to actually simulate the relaxation into the steady state.

The objects of interest are height fluctuation cumulants of the form

$$C_n(t)=\lim_{s\to\infty}\langle[h(x,t+s)-h(x,s) -\langle h(x,t+s)-h(x,s)\rangle]^n\rangle_c \tag{54}$$

and in particular their reduced amplitudes

$$\tilde{c}_n=\lim_{t\to\infty}\lim_{L\to\infty}(A^2|\lambda|t)^{-n/3}C_n(t)\ , \tag{55}$$

cf. (3) and (17). Obviously, the growth-rate corrections (5) are absent here. We have determined $\tilde{c}_2$ and $\tilde{c}_3$ from 200 runs in which a single-step interface of length $L=10\,000$, at zero tilt, was grown for 1000 time steps, and we estimate

$$\tilde{c}_2=0.712\pm0.003 \tag{56}$$

and

$$\tilde{c}_3=-0.199\pm0.004 \tag{57}$$

(recall that $\lambda=-1$ for this model). The skewness of the distribution is thus close to the value found in the transient case, $|s|\approx0.33$. The fact that $\tilde{c}_2>c_2$ is easily understood: The stationary average includes fluctuations in the initial conditions in addition to those generated in the growth process, and therefore the distribution of height fluctuations is expected to be broader. For the linearized KPZ equation a simple calculation shows that the ratio of the stationary to the transient amplitude equals $\sqrt{2}$.

The presence of fluctuations in the initial conditions has dramatic consequences if the interface is tilted. The gradient expansion of the inclination-dependent growth rate $v_\infty(u)$ leading to the KPZ equation (8) gives, in general, a linear term $v'_\infty(u)\nabla h$ where $v'_\infty(u)=-u$ for the single-step model. This term causes slope fluctuations to drift laterally along the interface. It is irrelevant, and therefore commonly transformed away, in the transient situation, but in the stationary case the drift allows the initial fluctuations to completely swamp those generated by the growth process [52]. As a consequence the second moment grows *linearly* in time,

$$C_2(t)=|v'_\infty|\,At+\mathcal{O}(t^{2/3}) \tag{58}$$

and the nontrivial scaling behavior appears only as a subleading correction. The leading behavior of (58) in fact does not depend on the presence of the nonlinearity in the KPZ equation (note that the amplitude is indepen-

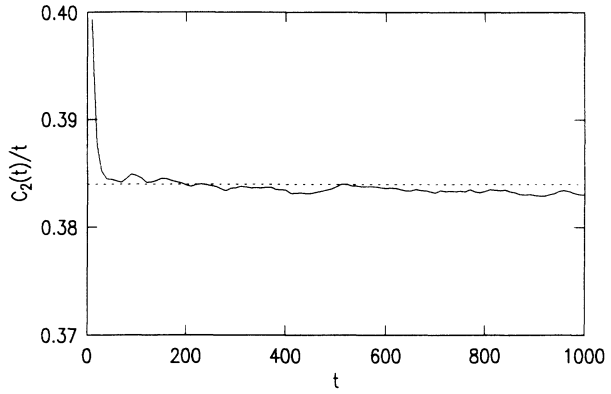

FIG. 13. Height fluctuations in the stationary state for the single-step model on an inclined substrate. The squared fluctuations increase *linearly* in time. The system size was $L=100\,000$, the tilt $u=0.6$, and the data are an average over 20 runs. The dotted line is the prediction (58) for the prefactor.

dent of λ), and can easily be derived from the linearized theory. We have checked the prediction (58) in a simulation at $u=0.6$ (Fig. 13).

VII. DISCUSSION AND CONCLUSION

The central result of this paper is the demonstration of amplitude universality for a large class of stochastic models of interface growth and directed polymers in random media. We reemphasize that the same values of the appropriately normalized amplitudes where found for *all* models we investigated. In this last section we summarize the current state of affairs regarding quantitative predictions of these amplitudes. Before doing so we discuss related numerical work on the subject.

In a study of crossover behavior in kinetic roughening, Guo, Grossmann, and Grant (GGG) [53] measured the λ dependence of the width prefactor, a_2, for a discretized version of the KPZ equation. They found $a_2 \sim \lambda^{0.46\pm0.04}$ in contrast with the scaling result $a_2 \sim \lambda^{2/3}$. Our results, displayed in Fig. 7, clearly support the scaling prediction (17). For comparison it should be noted that GGG varied λ by a factor of 2, while our work covers four orders of magnitude in the scaling parameter. Moreover, GGG used the bare value of λ, neglecting a possible renormalization due to the discretization scheme. Hence we expect that subsequent studies of the discretized KPZ equation will find agreement with our results.

Several very recent papers address questions concerning the probability distribution of height fluctuations, or free-energy fluctuations for the directed polymer [42,54–56]. Havlin *et al.* [54] presented numerical results for height fluctuations in ballistic deposition, and claimed the scaled distribution to be Gaussian *both* in the stationary ($t \gg L^z$) and the transient ($t \ll L^z$) regime. It is clear from our work that this can be true only in an approximate sense, for the simple reason that the transient distribution is skewed, as was observed by Halpin-Healy [42] and previously noted by Nattermann and Renz [43]. Kim, Moore, and Bray [55] studied the distribution of the ground-state energy in a zero-temperature directed-polymer simulation. They estimate the skewness $s=-0.29\pm0.02$ and the ratio $c_4/c_2^2 \approx 0.16$, both in good agreement with our estimates. Amar and Family [56] obtained $c_2=0.45\pm0.05$ from simulations of various growth models and $c_2 \approx 0.37$ from a numerical solution of the KPZ equation, both consistent with our results. They also estimated the static amplitude ratio $b_v/(\lambda b_2)=6.5\pm0.2$, in reasonable agreement with the exact value $b_v/(\lambda b_2)=6$ [cf. (13) and (14)].

Summarizing these remarks, we conclude that a coherent picture appears to be emerging on the numerical side. The theoretical situation is much less clear. In the context of the KPZ theory of kinetic roughening the only analytic amplitude predictions were made for the steady-state dynamic correlations discussed in Sec. VI [57]. Van Beijeren, Kutner, and Spohn (BKS) [27] derived a self-consistent integro-differential equation for the two-point correlation function within the mode-coupling approximation. Assuming a Gaussian shape for the universal scaling function, this leads to the prediction [36,29] $\tilde{c}_2=\sqrt{2/\pi}w^{-1}$, where w is the width of the Gaussian. A self-consistent determination of w gives $\tilde{c}_2=0.686$, while a perturbative calculation of the scaling function for small arguments [28] gives $\tilde{c}_2=0.74\pm0.01$, both rather close to our numerical estimate (56) [58]. Very recently Hwa and Frey [51] have argued that the BKS equation is an *exact* consequence of the dynamic renormalization group. They solved the equation numerically and obtained the estimate $\tilde{c}_2=0.69\pm0.01$, in good agreement with the earlier predictions [27,28] and our numerical value.

A different calculation of the stationary dynamic correlations was presented by Yakhot and She [59]. Their result implies $\tilde{c}_2=(2/\pi^2)^{2/3}\Gamma(\frac{1}{3})\approx0.924$, which is clearly ruled out by our numerics. This is not surprising, as the proposed form of the scaling function [59] is singular at the origin and hence is expected to be valid only for sufficiently large arguments.

A number of predictions for the universal amplitudes arise from the work of Kardar [9] and Bouchaud and Orland [41] in the context of directed polymers. These authors employ the replica trick, which means that averaged moments $\langle Z^n \rangle$ of the polymer partition function (42) are evaluated and then analytically continued to $n=0$. $\langle Z^n \rangle$ is related to the propagator of a quantum-mechanical system of n particles interacting through a pair potential given by the noise correlator (43). As the length of the polymer (the time t in the interface model) becomes large, the propagator is dominated by the ground-state energy, which takes a simple form for δ-function interactions. Expanding the asymptotic form for $\langle Z^n \rangle$ in n then yields expressions for the cumulants of the free energy, $-\ln Z$.

Proceeding along these lines, Kardar [9] found that the *third* cumulant is extensive (proportional to t), and concluded therefore that the free-energy exponent $\omega=\zeta/z=\frac{1}{3}$, in agreement with the KPZ result [1]. His prediction for the reduced amplitude of the third cumulant, in our units, is $c_3=-\frac{1}{4}$, which is clearly inconsistent

with our numerical estimates (though it does predict the correct sign). Moreover, the replica calculation implies that all higher cumulants vanish in the thermodynamic limit, $c_n=0$ for $n>3$, whereas we (as well as Kim, Moore, and Bray [55]) find evidence that $c_4>0$.

Bouchaud and Orland [41] (BO) refined Kardar's treatment by including the center-of-mass motion of the particle system in the evaluation of the quantum-mechanical propagator. Following a transformation to an equivalent toy model [60] of a Hookian spring subject to potential energy of Gaussian random slope, which is readily simulated, they arrive at the predictions $c_2=0.28$ and $c_v=-0.32$. Again, these values are nowhere near our numerical estimates. Halpin-Healy [42] found similarly poor agreement with the predictions [41] concerning the positional fluctuations of the polymer. Thus the claim of BO that their toy model "contains the full physics of the original problem" does not hold up to closer scrutiny.

While we hope that these discrepancies will be clarified by future work, we may tentatively attribute them to the breaking of replica symmetry [12,61] in the disordered polymer problem. It should be clear from our previous remarks that the replica calculations imply a nontrivial exchange of the limits $t\to\infty$ and $n\to 0$. Parisi [48] has recently argued that these limits do not commute in general, and that their failure to do so may change the values of amplitudes. Hence the amplitudes that we have determined could be useful in uncovering rather deep notions in the statistical mechanics of disordered systems. In that sense, they seem to carry much more information than the scaling exponents themselves, which appear to be rather robust with respect to such subtleties.

ACKNOWLEDGMENTS

We thank T. Hwa, M. Kardar, and H. Spohn for useful discussions, and T. Hwa, J. M. Kim, and J. G. Amar for making their work available to us prior to publication. This work was supported in part by grants from the Research Corporation and the Petroleum Research Fund, the latter being administered by the American Chemical Society.

APPENDIX: TIME-SCALE FLUCTUATIONS AND FINITE-SIZE EFFECTS

The following considerations apply to models in which the inclination dependence of the growth rate is due to a variation of the density of growth sites with inclination [25]. If the eligible growth sites are filled independently at unit rate, the growth rate is then proportional to the number of growth sites per projected substrate area. We use the single-step model [15,30] as an illustration, but we have observed similar effects in simulations of the restricted solid-on-solid model [20] and we expect them to occur in, e.g., the Eden model [62] as well.

We have shown in Sec. III that the density ρ of growth sites in the single-step model at zero tilt ($u=0$) equals $\frac{1}{4}$ in the thermodynamic limit. Here we are concerned with the leading correction to this value for a system of L sites with periodic boundary conditions. We will argue that the correction depends on the ensemble in which the average growth rate is evaluated, an effect which is important to take into account in numerical simulations. For simplicity we restrict ourselves to the case $u=0$. In terms of the spin representation introduced in Sec. III,

$$\rho=\tfrac{1}{4}(1-\langle\sigma_{x-1}\sigma_x\rangle) \tag{A1}$$

and the result $\rho=\frac{1}{4}$ follows from the independence of spins in the thermodynamic limit. In a finite system it is still true that all configurations with fixed magnetization (tilt) have the same weight in the stationary state [15]. For $u=0$ there are $L/2$ spin of each sign to be distributed on the lattice. A growth site is given by a pair $(\sigma_{x-1},\sigma_x)=(-1,1)$. For the first spin $\sigma_{x-1}=-1$, there are L positions available. However, once the first spin is fixed, there are only $L-1$ positions available to place one of the $L/2+$spins. This implies a negative correlation

$$\langle\sigma_x\sigma_y\rangle=-\frac{1}{(L-1)} \tag{A2}$$

for $x\neq y$, which is in fact *independent* of the distance between the spins. Thus

$$\rho=\tfrac{1}{4}\left[1+\frac{1}{L-1}\right]. \tag{A3}$$

Using (25) and (26) this is verified to agree, to leading order in $1/L$, with the general expression (14) [24].

To correctly generate the stationary state of the continuous time stochastic process which defines the single-step model, it is important that *time* in a simulation be counted as the number of *attempted depositions* per site. In an elementary simulation step a site is picked at random, deposition is attempted, and time is increased by $1/L$ independent of the success of the attempt. On this time scale the deposit thickness (number of successful depositions per substrate site) becomes a fluctuating quantity. From the point of view of computational efficiency it is natural to avoid unsuccessful attempts by keeping a *list* of eligible growth sites and making a random choice only among these. Time is then equal to the deposit thickness which does *not* fluctuate. A moments thought reveals that this procedure, referred to as the *list algorithm* in the following, defines a new dynamical ensemble in which configurations with many growth sites carry more weight [63]. To investigate this effect quantitatively we introduce the number $C(L,M)$ of configurations with zero tilt and M growth sites in a system of size L [64]. Here $M=1,\ldots,L/2$ and the total number of configurations is

$$\mathcal{C}(L)=\sum_{M=1}^{L/2}C(L,M)=\binom{L}{L/2} \tag{A4}$$

In the ensemble where each configuration has the same weight the probability distribution for the number of growth sites is simply $P(M)=C(L,M)/\mathcal{C}(L)$, the first moment of which is $\langle M\rangle=\rho L$. In contrast, the dynamic ensemble generated by the list algorithm is readily seen to give rise to the distribution

$$\tilde{P}(M)=\frac{M}{\langle M\rangle}P(M)\ , \tag{A5}$$

i.e., the probability to find M growth sites is multiplied by M. While we have not been able to explicitly calculate the $C(L,M)$, we observe by exact numerical enumeration up to $L=16$ that the distribution (A5) is *symmetric* for all L. Its first moment is therefore $(L/2+1)/2$, and the density of growth sites evaluated in this ensemble is

$$\tilde{\rho}=\tfrac{1}{4}\left[1+\frac{2}{L}\right] \tag{A6}$$

with a leading correction term that differs from (A3). We note that it is possible to incorporate the correct time-scale fluctuations into the list algorithm by increasing time by the inverse of the actual number of growth sites at each deposition step [65]. The growth rate measured in such a way is

$$v=\frac{2}{L\langle 1/M\rangle_{\sim}}=\frac{2\langle M\rangle}{L}=2\rho\ , \tag{A7}$$

where $\langle\ \rangle$ and $\langle\ \rangle_{\sim}$ denote averages obtained using the distribution P and $\tilde{P}$, respectively.

[1] M. Kardar, G. Parisi, and Y. C. Zhang, Phys. Rev. Lett. **56**, 889 (1986).

[2] Some recent reviews are J. Krug and H. Spohn, in *Solids Far From Equilibrium: Growth, Morphology and Defects*, edited by C. Godrèche (Cambridge University Press, Cambridge, 1991); J. Krug, *Die Entstehung fraktaler Oberflächen* (Harri Deutsch, Frankfurt, 1990); F. Family, Physica A **168**, 561 (1991); *Dynamics of Fractal Surfaces*, edited by F. Family and T. Vicsek (World Scientific, Singapore, 1991).

[3] T. Vicsek, *Fractal Growth Phenomena* (World Scientific, Singapore, 1989).

[4] J. Villain, J. Phys. Fr. I **1**, 19 (1991).

[5] P. Meakin, CRC Crit. Rev. Solid State Mater. Sci. **13**, 143 (1987).

[6] M. A. Rubio, C. A. Edwards, A. Dougherty, and J. P. Gollub, Phys. Rev. Lett. **63**, 1685 (1989); V. K. Horváth, F. Family, and T. Vicsek, J. Phys. A **24**, L25 (1991); J. Krug and P. Meakin, Phys. Rev. Lett. **66**, 703 (1991).

[7] J. Krug and P. Meakin, Phys. Rev. A **40**, 2064 (1989), and references therein.

[8] M. Kardar and Y. C. Zhang, Phys. Rev. Lett. **58**, 2087 (1987).

[9] M. Kardar, Nucl. Phys. B **290**, 582 (1987).

[10] B. Derrida, Physica A **163**, 71 (1990), and references therein.

[11] T. Halpin-Healy, Phys. Rev. A **42**, 711 (1990).

[12] M. Mézard and G. Parisi, J. Phys. Fr. I **1**, 809 (1991).

[13] F. Family and T. Vicsek, J. Phys. A **18**, L75 (1985); R. Jullien and R. Botet, *ibid.* **18**, 2279 (1985).

[14] R. Lipowsky, in *Fundamental Problems in Statistical Mechanics VII*, edited by H. van Beijeren (North-Holland, Amsterdam, 1990).

[15] P. Meakin, P. Ramanlal, L. M. Sander, and R. C. Ball, Phys. Rev. A **34**, 5091 (1986).

[16] J. Krug, Phys. Rev. A **36**, 5465 (1987).

[17] E. Medina, T. Hwa, M. Kardar, and Y. C. Zhang, Phys. Rev. A **39**, 3053 (1989).

[18] D. Forster, D. R. Nelson, and M. J. Stephen, Phys. Rev. A **16**, 732 (1977).

[19] D. A. Huse, C. L. Henley, and D. S. Fisher, Phys. Rev. Lett. **55**, 2924 (1985).

[20] J. M. Kim and J. M. Kosterlitz, Phys. Rev. Lett. **62**, 2289 (1989).

[21] B. M. Forrest and L.-H. Tang, Phys. Rev. Lett. **64**, 1405 (1990).

[22] T. Hwa (private communication).

[23] For a random variable with zero mean the first three cumulants are equal to the moments $\langle X^n\rangle_c=\langle X^n\rangle$ for $n=1,2,3$, and the fourth cumulant is $\langle X^4\rangle_c=\langle X^4\rangle-3\langle X^2\rangle^2$.

[24] J. Krug and P. Meakin, J. Phys. A **23**, L987 (1990).

[25] J. Krug, J. Phys. A **22**, L769 (1989).

[26] M. Plischke and Z. Rácz, Phys. Rev. A **32**, 3825 (1985).

[27] H. van Beijeren, R. Kutner, and H. Spohn, Phys. Rev. Lett. **54**, 2026 (1985).

[28] H. K. Janssen and B. Schmittmann, Z. Phys. B **63**, 517 (1986).

[29] See also J. Krug in Ref. [2].

[30] M. Plischke, Z. Rácz, and D. Liu, Phys. Rev. B **35**, 3485 (1987).

[31] D. J. Gates and M. Westcott, Proc. R. Soc. London Ser. A **416**, 443 (1988); **416**, 463 (1988); D. J. Gates, J. Stat. Phys. **52**, 245 (1988).

[32] S. Katz, J. L. Lebowitz, and H. Spohn, J. Stat. Phys. **34**, 497 (1984).

[33] H. Brandstetter, Diploma thesis, University of Munich 1990 (unpublished).

[34] J. G. Amar and F. Family, Phys. Rev. Lett. **64**, 543 (1990); J. Krug and H. Spohn, *ibid.* **64**, 2232 (1990).

[35] W. van Saarloos and G. H. Gilmer, Phys. Rev. B **33**, 4927 (1986), and references therein.

[36] J. Krug and H. Spohn, Europhys. Lett. **8**, 219 (1988).

[37] D. E Wolf, J. Phys. A **20**, 1251 (1987).

[38] J. Krug and H. Spohn, Phys. Rev. A **38**, 4271 (1988).

[39] M. Kardar, Phys. Rev. Lett. **55**, 2923 (1985).

[40] D. A. Huse and C. L. Henley, Phys. Rev. Lett. **54**, 2708 (1985).

[41] J. P. Bouchaud and H. Orland, J. Stat. Phys. **61**, 877 (1990).

[42] T. Halpin-Healy, Phys. Rev. A **44**, R3415 (1991).

[43] T. Nattermann and W. Renz, Phys. Rev. B **38**, 5184 (1988).

[44] In the growth model context the natural analog of this initial condition is the growth from a point seed rather than from a substrate.

[45] This geometry was employed in the recent zero-temperature DPRM simulations of Kim, Bray, and Moore [55].

[46] In the terminology of first-passage percolation, which is an equivalent formulation of the zero-temperature DPRM (see H. Kesten, Ann. Prob. **15**, 1231 (1987) for a review, and J. Krug and H. Spohn in [2] for a brief discussion of the relation to growth models and DPRM), $Z(x,t)$ is a

point-to-point partition function (all paths share the same starting *and* end point), while $\mathcal{Z}(t)$ is a *point-to-line* quantity. Though it can be shown that the averages of $F=-\ln Z$ and $\mathcal{F}=-\ln\mathcal{Z}$ agree to leading order in t, the finite-size corrections and fluctuations may be expected to differ in the two cases. Our preliminary numerical results indicate that F and $\mathcal{F}$ are characterized by the same scaling exponents but *different* amplitudes.

[47] J. Cook and B. Derrida, J. Stat. Phys. **63**, 505 (1991), compute finite-size corrections for the mean-field version of the DPRM.

[48] G. Parisi, J. Phys. Fr. **51**, 1595 (1990).

[49] M. Mézard, J. Phys. Fr. **51**, 1831 (1990).

[50] In the context of growth models the use of inhomogeneous macroscopic profiles to extract parameters like λ was proposed by D. E. Wolf and L.-H. Tang, Phys. Rev. Lett. **65**, 1591 (1990).

[51] T. Hwa and E. Frey (unpublished).

[52] H. van Beijeren, J. Stat. Phys. **63**, 47 (1991) investigated the relative importance of initial and kinetically generated fluctuations in the equivalent [36] case of one-dimensional driven diffusive systems [27,28]. For a brief discussion in the interface context see Chap. 6 of the review article by J. Krug and H. Spohn in [2].

[53] Hong Guo, B. Grossmann, and M. Grant, Phys. Rev. A **41**, 7082 (1990).

[54] S. Havlin, S. V. Buldyrev, H. E. Stanley, and G. H. Weiss, J. Phys. A **24**, L925 (1991).

[55] J. M. Kim, M. A. Moore, and A. J. Bray, Phys. Rev. A **44**, 2345 (1991).

[56] J. G. Amar and F. Family (unpublished).

[57] Amar and Family [56] quote a result obtained from the one-loop renormalization calculation of KPZ [1], $c_2\approx 0.57$, which presumably also refers to the steady-state situation.

[58] In [36] this result was erroneously applied to the transient case.

[59] V. Yakhot and Z. S. She, Phys. Rev. Lett. **60**, 1840 (1988).

[60] J. Villain, B. Semeria, F. Lanon, and L. Billard, J. Phys. C **16**, 2588 (1983); U. Schultz, J. Villain, E. Brézin, and H. Orland, J. Stat. Phys. **51**, 1 (1988).

[61] The applicability of the concept of replica symmetry breaking in this context (and in general) was recently challenged by D. S. Fisher and D. A. Huse, Phys. Rev. B **43**, 10 728 (1991).

[62] R. Hirsch and D. E. Wolf, J. Phys. A **19**, L251 (1986).

[63] This observation was independently made by H. C. Kang and J. W. Evans, Phys. Rev. A **44**, 2335 (1991).

[64] In the spin language, $C(L,M)$ is the number of Ising configurations with fixed magnetization *and* fixed energy.

[65] A similar definition of time is used in simulations of diffusion-limited reaction kinetics; see, e.g., D. Ben-Avraham, J. Stat. Phys. **48**, 315 (1987).